

Supporting information
Nb₃O₇F Mesocrystals: Orientation Formation and Application in Lithium
Ion Capacitors

Zhijie Chen, Zhiwei Li, Wenjie He, Yufeng An, Laifa Shen, Hui Dou, and Xiaogang Zhang*

Jiangsu Key Laboratory of Electrochemical Energy Storage Technologies, College of Materials Science and Engineering, Nanjing University of Aeronautics and Astronautics, Nanjing, 210016, P.R. China.

*Corresponding author

E-mail: azhangxg@163.com (X.G. Zhang)

1. Material characterization

The phase and crystal structures of NOF-NCMs were analysed by X-ray diffraction (XRD, Bruker D8 advance X-Ray Diffractometer) with Cu K α radiation ($\lambda = 1.5406 \text{ \AA}$). The microstructures of as-synthesized samples were characterized by the field-emission scanning electron microscopy (FESEM, HITACHI S-4800), transmission electron microscopy (TEM, FEI, Tecnai-20) and high-resolution transmission electron microscopy (HRTEM, JEOL JEM-2010). The selective area electron diffraction (SAED) patterns were attached to HRTEM. The compositions of the as-synthesized samples were characterized by the energy dispersive X-ray spectroscopy (EDS) technology. The surface areas of as-synthesized samples were determined by Brunauer-Emmett-Teller (BET) measuring method (ASAP-2010 surface area analyser).

2. Electrochemical measurements

Typically, the electrochemical properties were tested by galvanostatic technique in a CR2016-type coin cell battery. For NOF-NCMs and bulk Nb₃O₇F electrode, 70 wt.% electro-active material (NOF-NCMs or bulk Nb₃O₇F), 20 wt.% conductive additive (acetylene black; KJ group, batch number: 0011910) and 10 wt.% polymer binder (polyvinylidene difluoride, PVDF; KJ group, batch number: 0011609) were dissolved together in organic solvent (N-methyl pyrrolidinone, NMP), milled for 30 minutes in an agate mortar to make them to be homogeneously mixed, pasted on a Cu foil current collector and then dried at 110 °C in vacuum for 12 h. For AC (YP-80F; Kuraray) electrode, its electrode preparation process is almost the same to that of anode except that its electrode pulp ratio changes into 80 : 10 : 10. In the above mentioned electrode, Li metal was served as both the reference and the counter electrodes. The polypropylene (PP) film was chosen as a separator and 1.0 M LiPF₆ solution in a 1 : 1 (volume ratio) mixture of dimethyl carbonate (DMC) and ethylene carbonate (EC) was used as electrolyte. The assembly process of all coin cells was in an argon-filled glove box.

Before constructing a LIC device, a pre-lithiation process should be taken place in the NOF-NCMs anode. A short connection method is applied for pre-lithiation process. Typically, the NOF-NCMs electrode and lithium foil were directly attached in the same electrolyte by short circuiting and the pre-lithiation process can be completed after standing for 12 h. Next, the pre-lithiated NOF-NCMs anode was cleared with EC organic solution and shifted to the fabrication of LIC full cell. The mass ratio between pre-lithiated anode and cathode is fixed as 1 : 3.

All the cells were galvanostatically charged and discharged (GCD) at different current densities using a CT2001A cell testing equipment (LAND Electronic Co.). Cycling voltammetry (CV) and electrochemical impedance spectroscopy (EIS) technology were tested by an electrochemical workstation (CH Instruments, model 660C). EIS data can be obtained at open circuit potential after first GCD cycle. And its characteristic frequency is 0.01-100000Hz.

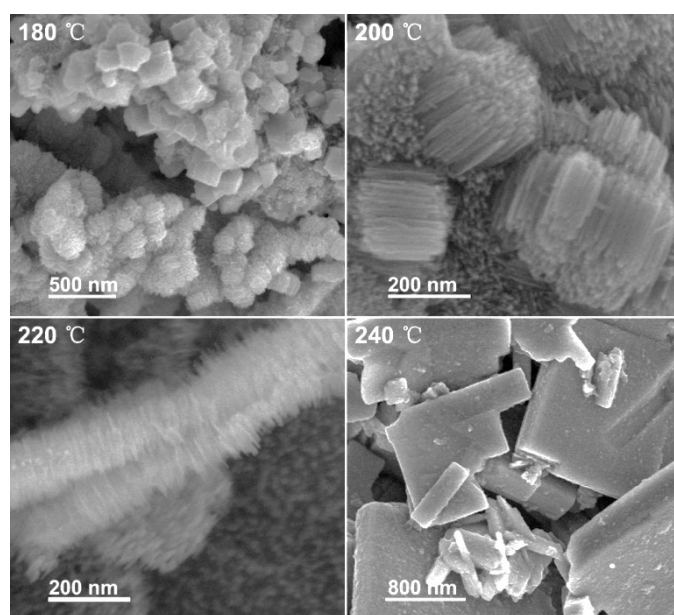


Fig. S1 The FESEM images of obtained products of different temperature (other reaction conditions: 0.36 g NbCl_5 , 20 mL isopropanol, 200 μL HF, 30 μL HCl, 24 h).

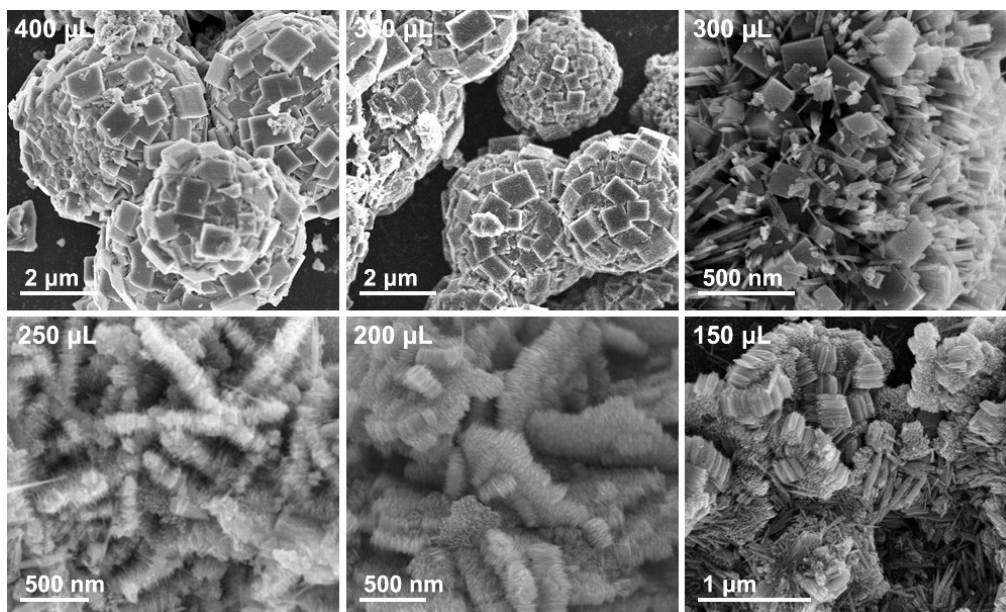


Fig. S2 The FESEM images of obtained products of different concentrations of HF (other reaction conditions: 0.36 g NbCl_5 , 20 mL isopropanol, 30 μL HCl, 220 °C, 24 h).

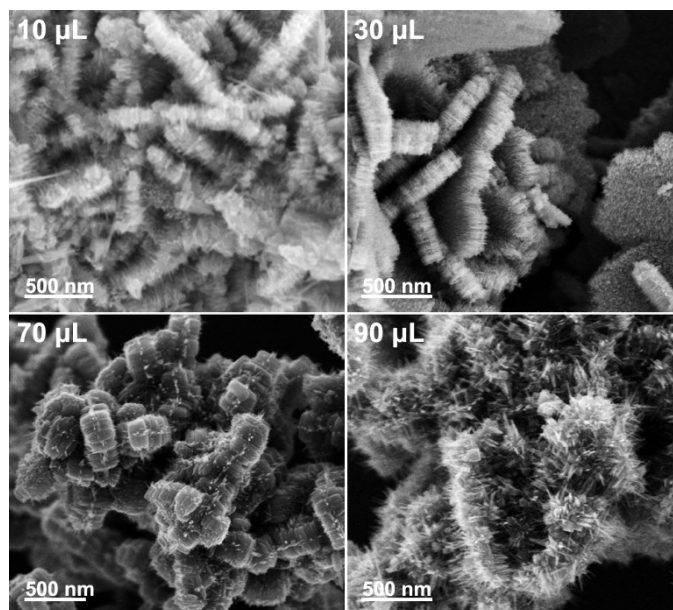


Fig. S3 The FESEM images of obtained products of different concentrations of HCl (other reaction conditions: 0.36 g NbCl₅, 20 mL isopropanol, 200 μL HF, 220 °C, 24 h).

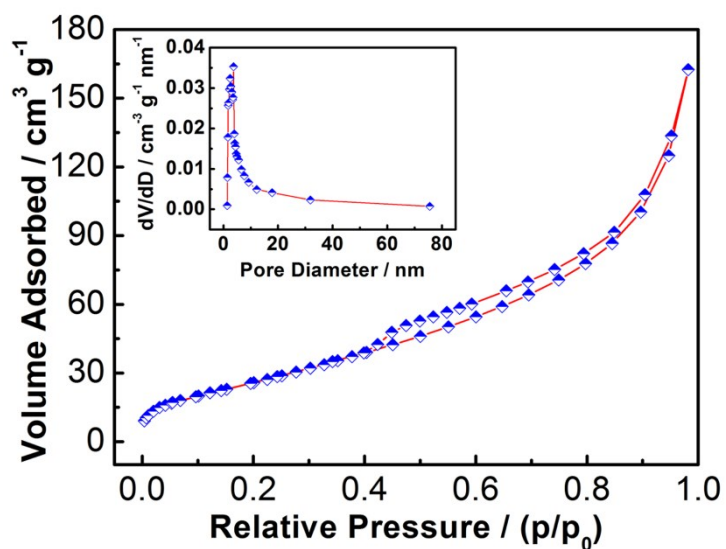


Fig. S4 N₂ adsorption-desorption isotherms pattern and the corresponding pore size distribution pattern (insert) of NOF-NCMs.

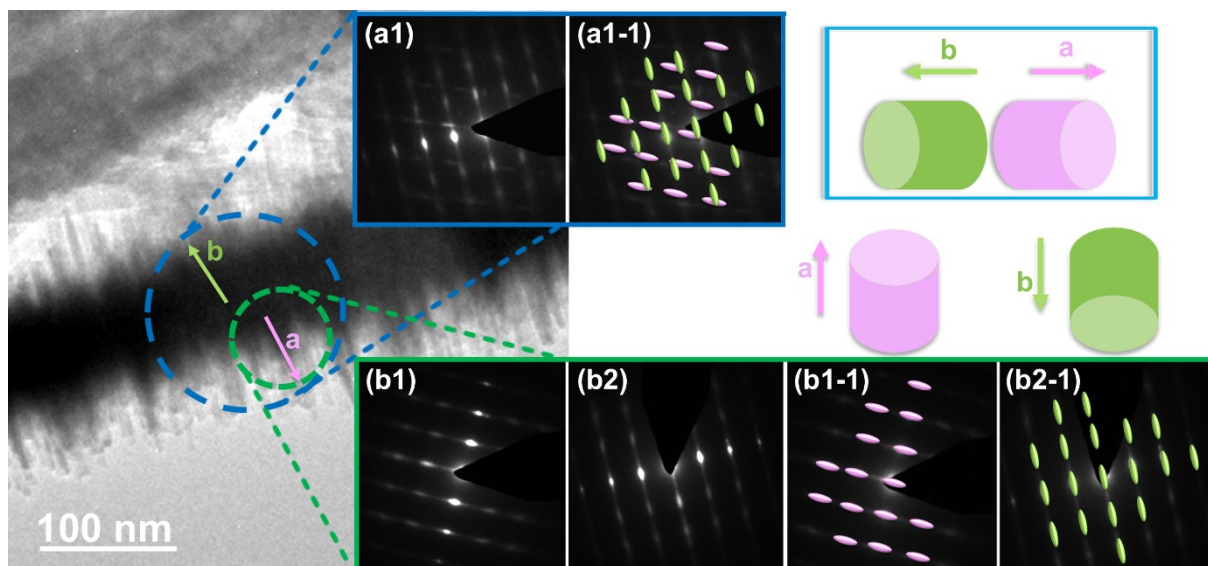


Fig. S5 Classical HRTEM images and SAED (insert) patterns of NOF-NCMs (In **Fig. S5**, the SAED pattern for blue circle is denoted as SAED-a1 while for green circle is denoted as SAED-b1. SAED-b2 is obtained by rotating SAED-b1. The SAED-b1-1 can be obtained by replacing the original light spot with the pink spot. Similarly, the SAED-b2-1 can be obtained by replacing the original light spot with the green spot. Overlap the pink dot with the green dot to cover up the original light dot of SAED-a1, thus SAED-a1-1 is obtained.)

The difference between SAED-b1-1 and SAED-b2-1 can be regarded as the different angle of detection light. Actually, in the same test, the angle of detection light is fixed. Therefore, the different angle of detection light can be due to that the placement angle of corresponding nanowires is different. Based on this, SAED-b1-1 can stand for growth direction a while SAED-b2-1 can represent growth direction b. For SAED-a1-1, two sets of light spot arrays imply two kinds of placement angle of corresponding nanowires. As a result, SAED-a1-1 can both contain two growth directions, as shown in **Fig. S5**. This implying that the macroscopic growth mechanism is to start growing from both sides of reaction precursors.

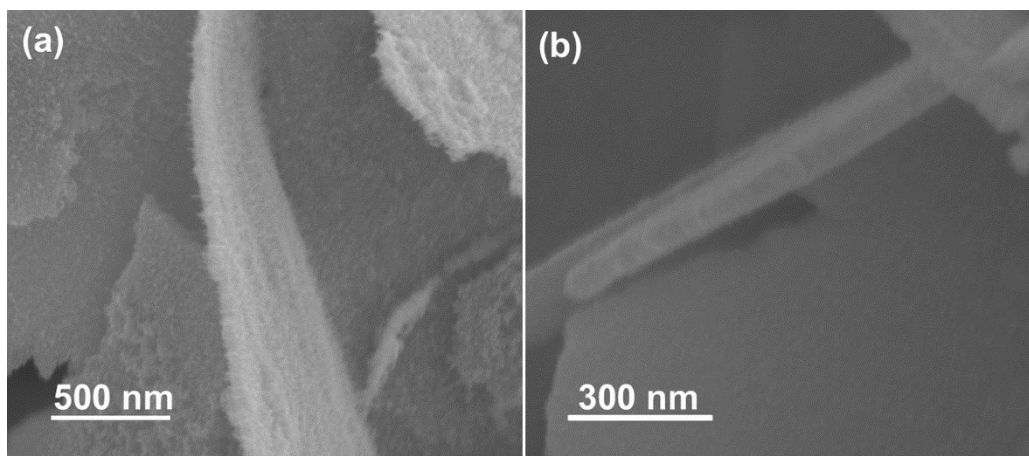


Fig. S6 The FESEM images of obtained products of 30 μL (a) HNO_3 and (b) H_2SO_4 (other reaction conditions: 0.36 g NbCl_5 , 20 mL isopropanol, 200 μL HF, 220 $^\circ\text{C}$, 24 h).

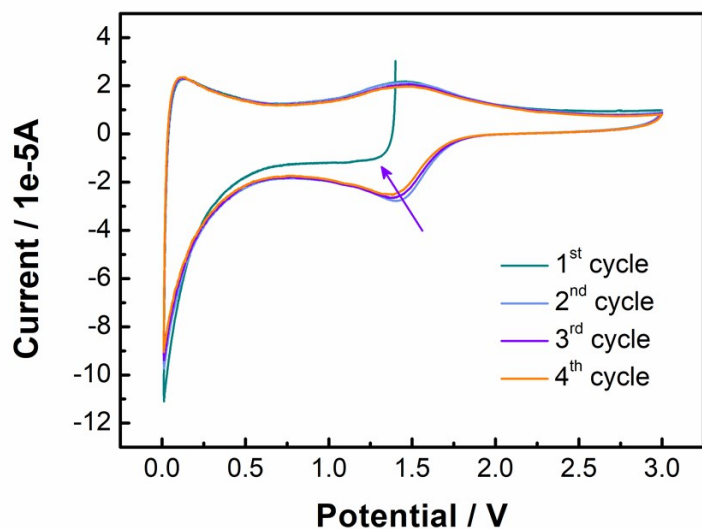


Fig. S7 CV curves of NOF-NCMs at 0.1 mV s^{-1} .

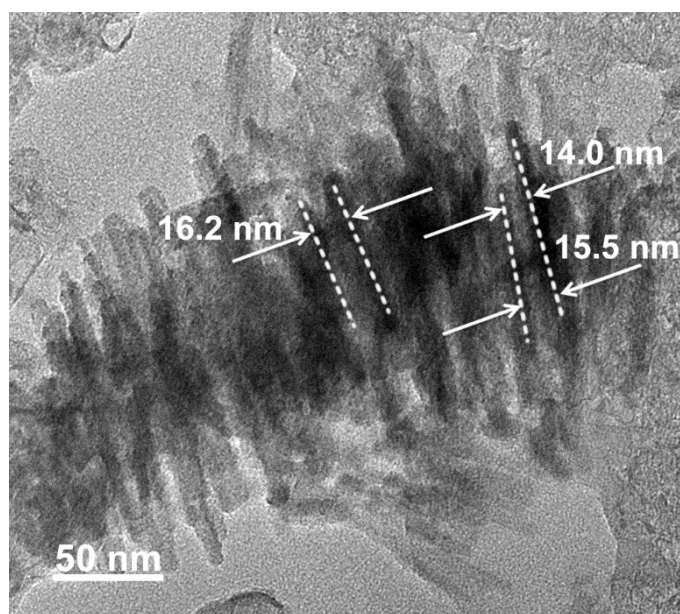


Fig. S8 The TEM images of NOF-NCMs after 1000 cycles charging and discharging process.

Seen from **Fig. S4**, the main pore sizes of NOF-NCMs are smaller than 5 nm. Since there are no obvious pore structures observed in each nanowire subunit (**Fig. 2d**), the sizes of these pore structures could be associated with the distance between adjacent nanowires. **Fig. S8** shows the TEM image of NOF-NCMs after finishing cycling test, presenting that the overall microstructure does not obviously change except that the distance between some of adjacent

nanowires is significantly larger than 10 nm. Therefore, we conclude that the distance between some of the adjacent nanowires will gradually enlarge during the charging-discharging process until it reaches a certain degree. However, the microstructure still maintain nanowires clusters, demonstrating its structure stability and thus cycling stability.

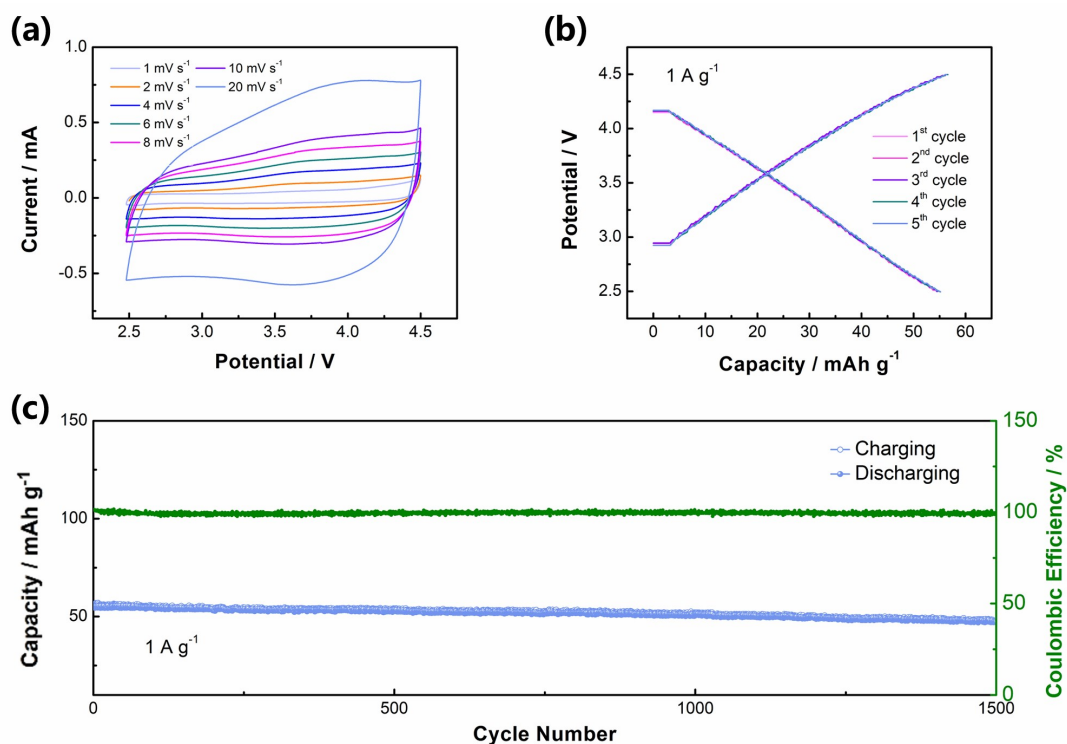


Fig. S9 Electrochemical performance of commercial AC: (a) The CV curves at different scan rates; (b) GCD curves for first five cycles; (c) Cycling performance at 1 A g⁻¹.

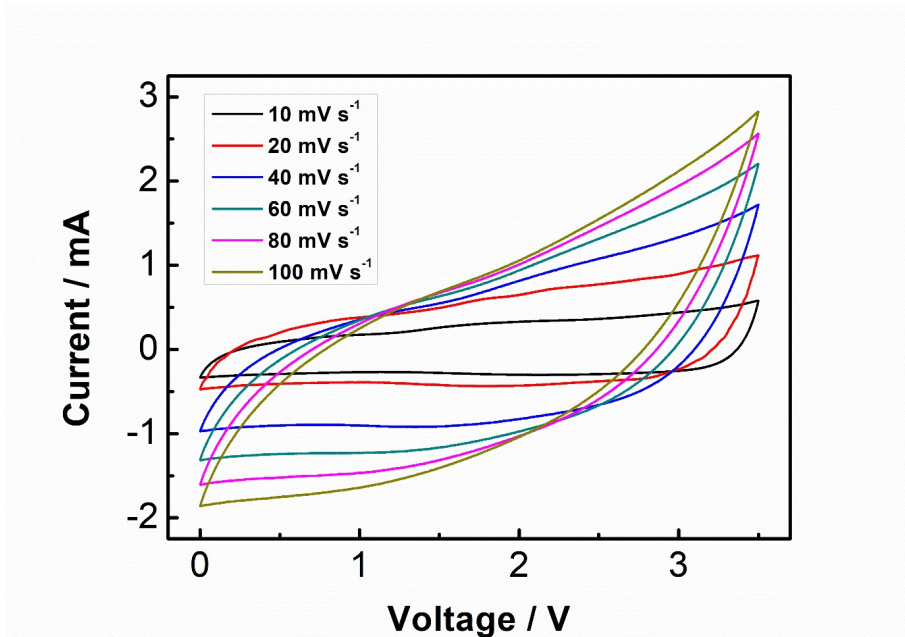


Fig. S10 CV curves of NOF-NCMs//AC LIC at the scan rate range of 10-100 mV s^{-1} .

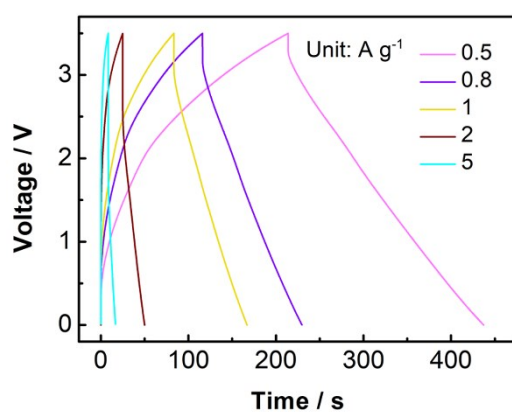


Fig. S11 GCD curves of NOF-NCMs//AC LIC at different current densities.

Table S1 The comparisons among the state-of-the-art anode materials.

Anode Materials	Morphology	Capacities, mA h g ⁻¹ (current density, mA g ⁻¹)	Average Potential	Capacity Retention (cycling number; current density, mA g ⁻¹)	Ref.
TiO ₂ Mesocrystals	Cube-like	227 (85)	1.75 V	83.8% (800 cycles; 850)	51
Li ₄ Ti ₅ O ₁₂	Nanotubes	183.1 (17.5)	1.60 V	89.0% (100 cycles; 17.5)	52
Nb ₂ O ₅	Microspheres	199 (100)	1.50 V	94.0% (150 cycles; 500)	53
TiNb ₂ O ₇	Nanofibers	284 (38.7)	1.65 V	92.0% (50 cycles; 3870)	54
LiNb ₃ O ₈	Porous nanofiber	240.7 (38.9)	1.25 V	70.6% (100 cycles; 38.9)	55
Fe ₃ O ₄	Nanowires	2416 (50)	0.75 V	63.7% (100 cycles; 50)	56
α-Fe ₂ O ₃	Hollow spheres	1702 (50)	0.95 V	57.4% (50 cycles; 50)	57
MoO ₃	Porous film	1286 (70)	0.75 V	81.8% (50 cycles; 70)	58
MoS ₂	Nanotubes	1487 (100)	0.50 V	76.5% (100 cycles; 500)	59
SnO ₂	Hollow spheres	1600 (100)	0.50 V	43.4% (50 cycles; 100)	60
NOF-NCMs	Nanowires	356.7 (100)	0.45 V	88.3% (3000 cycles; 800)	

Table S2 Possible conversion reactions.

Reaction
$\text{Nb}_3\text{O}_7\text{F} + 9\text{Li}^+ + 9\text{e}^- \rightleftharpoons 3\text{NbO} + 4\text{Li}_2\text{O} + \text{LiF}$
$\text{Nb}_3\text{O}_7\text{F} + 8\text{Li}^+ + 8\text{e}^- \rightleftharpoons 2\text{NbO} + 4\text{Li}_2\text{O} + \text{NbOF}$
$\text{Nb}_3\text{O}_7\text{F} + 5\text{Li}^+ + 5\text{e}^- \rightleftharpoons 3\text{NbO} + 2\text{Li}_2\text{O}_2 + \text{LiF}$
$\text{Nb}_3\text{O}_7\text{F} + 4\text{Li}^+ + 4\text{e}^- \rightleftharpoons 2\text{NbO} + 2\text{Li}_2\text{O}_2 + \text{NbOF}$